Fiber Optic Pore Pressure Sensor Development

B. G. GROSSMAN, P. J. COSENTINO, E. H. KALAJIAN, G. KUMAR, S. DOI, J. VERGHESE, AND P. LAI

Low-cost fiber optic sensors capable of measuring loads and pressures, including pore water pressures, have been developed. These sensors employ microbend fiber optic technology and are capable of measuring pressures from 0 to about 700 kPa (100 psi). They are relatively inexpensive and give reliable and repeatable results. A calibration setup was developed to ensure reliable data acquisition during load or pressure testing of microbend sensors. Sensor development and operation, along with their sensitivities, are described. The preferred configuration could be placed in the soil and used for the in situ monitoring of pore water pressures and total stresses once the development is completed.

In situ pore water pressures are a key to understanding soil behavior. The instruments currently used for monitoring these pressures include vibrating-wire piezometers, electrical resistance piezometers, pneumatic piezometers, and piezocones. They can be expensive and require special manufacturing techniques to control problems such as corrosion, zero drift of the output, power fluctuations, and low electrical output (*1*). If properly installed, they perform well but their long-term stabilities can be uncertain.

Prototype fiber optic sensors have been developed for measuring pore water pressures and loads under laboratory conditions. Loads up to 2.2 kg (5 lb) were measured with a bridge architecture sensor, and after modifying this sensor, pressures up to 700 kPa (100 psi) were measured by using the recommended pore pressure sensor configuration. The sensors give accurate, repeatable results and would cost about $100 to construct. To properly evaluate the sensors, a fiber optic load and pressure calibration system was assembled at Florida Tech (*2*).

OPTICAL FIBER SENSORS

Optical fibers were developed as a substitute for copper wires for use in high-speed and long-distance communications systems. It was recognized that they could be used as sensors if a change in the environment surrounding the fiber resulted in a change in the fiber's light transmission characteristics. For communication applications, this interaction is minimized by the cable surrounding the fiber. Developments in fiber optic sensor technology have led to its use in medicine, robotics, aviation, guidance and navigation systems, and sonar and seismic systems.

B. G. Grossman, S. Doi, and J. Verghese, Department of Electrical Engineering, Florida Institute of Technology, Melbourne, Fla. 32901-6988. P. J. Cosentino, E. H. Kalajian, and G. Kumar, Department of Civil Engineering, Florida Institute of Technology, Melbourne, Fla. 32901-6988. P. Lai, Florida Department of Transportation, 605 Suwannee Street, Tallahassee, Fla. 32399-0450.

Figure 1 shows a typical optical fiber consisting of a glass or plastic core, a cladding layer, an acrylic buffer, and one or more protective layers. Light is coupled or focused into one end of the fiber and travels through the core. The cladding keeps the light within the core, and the protective plastic layers that surround the cladding protect the fragile core and cladding. The protective plastic also allows the optical fiber to be flexible and durable. The core and cladding usually consist of highly transparent glass for telecommunication applications, but they may be made of clear plastic. Optical fibers are typically encased within multiple layers of high-strength plastics or other materials to form a rugged cable. The glasses used in optical fiber cores behave elastically up to their breaking points under tension, with Young's moduli ranging from 61,000 to 91,000 MPa (8.8 to 13.2 ksi) and Poisson's ratio ranging from 0.14 to 0.26 (*3*).

When a fiber optic sensing system is being developed, a number of components are required to generate, focus, detect, and record the light passing through the fiber sensing region. Lasers or light-emitting diodes (LEDs) can be used as light sources. The light output from the sensor can be detected with photodetectors. To obtain a uniform distribution of light in a multimode fiber core, a mode scrambler can be constructed by wrapping the fiber approximately 20 times around a rod 5 mm (0.20 in.) in diameter rod. Light can be removed from the cladding by applying an index matching material to a section of bare fiber core.

Over the last three decades fiber optic sensors have been developed for measuring temperature changes, chemical concentrations, stress, strain, load, and deflections (*4*). These sensors have significant advantages over the current sensors, including immunity to corrosion and electromagnetic interference and the ability to remotely sense parameters; in addition, multiple sensors can be placed in series on one fiber (i.e., multiplexing) (*5,6*).

FIBER OPTIC SENSOR CALIBRATION SYSTEM

The selection of an appropriate testing system and procedure was critical for studying the relationship between changes in load or pressure and light output intensity for the various optical fiber sensors. The system (Figure 2) consists of an LED to provide the input light, a mode scrambler to distribute the light throughout the core, either a compression machine to apply forces or a pressure chamber to apply pressures, a mode stripper to give accurate light output intensities, and a photodiode to measure the light output intensity. A data acquisition system was used to record the analog signals from the load cell or pressure transducer and the optical detector. A computer program was written to reduce the data to load or pressure versus light intensity. A step-by-step pro-

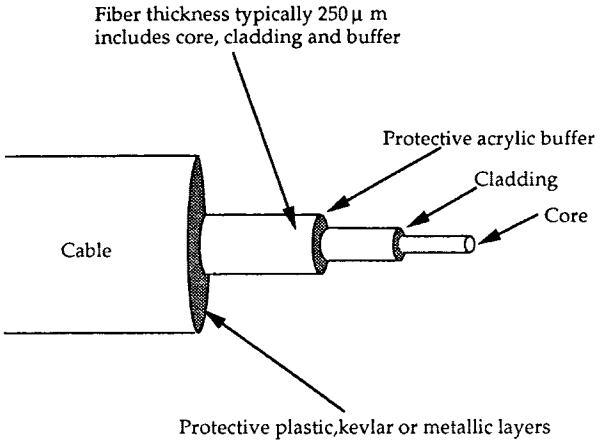

FIGURE 1 Typical optical fiber wrapped in a cabling material.

cedure for testing and calibrating the fiber optic sensors is given by Kumar (*2*).

LOAD AND PRESSURE FIBER OPTIC SENSOR DEVELOPMENT

After studying the advantages and disadvantages of the various types of fiber optic sensors, it was decided that microbend-type sensors would be the best choice for use in construction and testing. Figure 3 illustrates the concept of microbending for a fiber optic sensor. When a fiber is subjected to microbending along its axis, the light propagating through the core becomes unguided (i.e., leaks out), thereby decreasing the light intensity at the fiber's output. When a microbend sensor is used to measure loads or pressures, a calibration must be developed to give the relationship between the percentage of light lost and the corresponding load or pressure. During the present study, both load and pressure versus output light intensity curves were developed.

Numerous microbend sensor configurations were developed and tested by Kumar (*2*). His major findings and problems were that (a) the fiber would slip within the mechanical components of the microbend sensor, (b) the fiber was damaged or broken during some types of microbend testing, and (c) a system hysteresis occurred as the various sensors were loaded and unloaded (*2*).

The mechanical components of the sensors that cause microbending also caused the optical fibers to move or slip during testing. This slippage resulted in inconsistent results. To alleviate slippage a pretensioning apparatus, consisting of a series of springs and pulleys, was devised to pretension the fiber before testing. The pretensioning loads, which ranged from 0.25 kg (0.55 lb) to 2.0 kg (4.4 lb), resulted in sensor failure after very few load-unload repetitions, indicating that pretensioning was not the best approach available for the prevention of slippage (*2*).

During testing of some of the microbend sensors, there was visual evidence of optical fiber damage. The researchers inspected the fibers after each series of tests, and visual damage in the form of indentations in the fiber coating was noted. It was therefore decided to study how the optical fibers responded to direct applications of loads. Fibers were placed horizontally on a flat brass

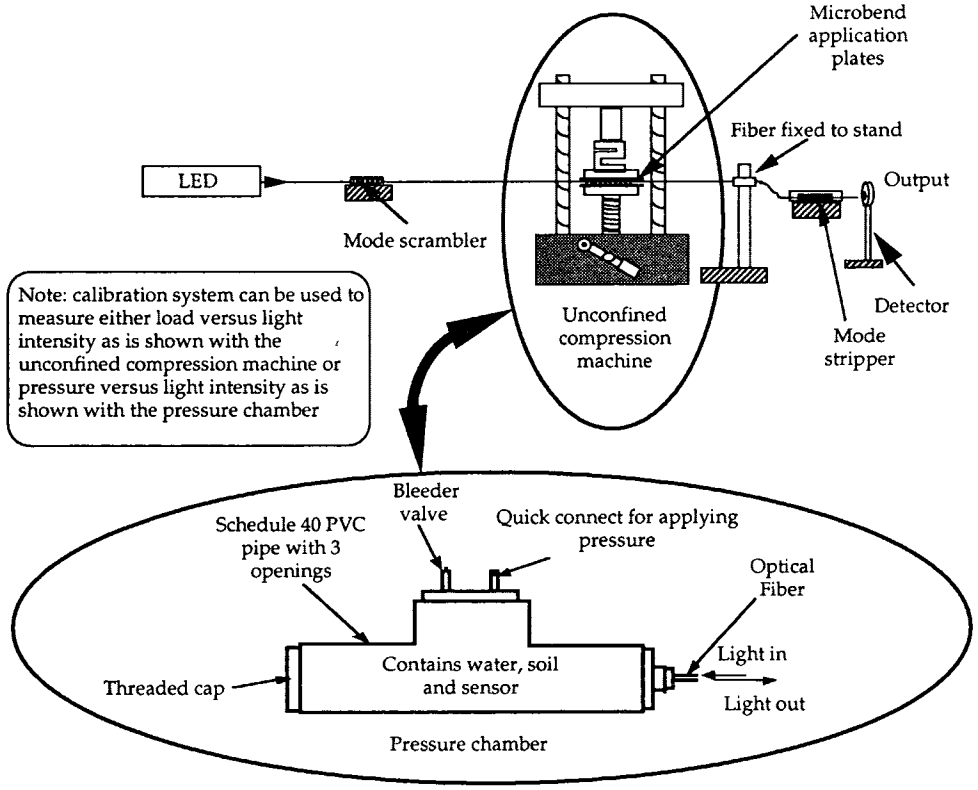

FIGURE 2 Force or pressure calibration system. PVC is polyvinyl chloride.

During microbending (from loads, pressures, etc.) light travelling within the fiber core leaks out. A powermeter is used to measure the remaining light at the sensor's output end and a calibration is developed between the load, pressure, etc., and the amount of output light.

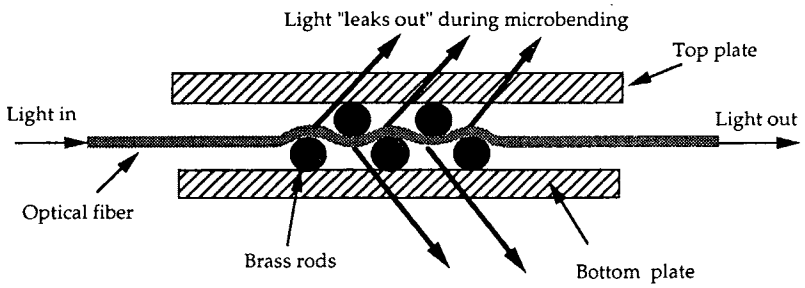

FIGURE 3 Brass plate sensor complying with breaking the radius requirement (not to scale).

plate, and forces were applied perpendicular to the fibers' longitudinal axes by using small-diameter brass rods at known spacings. Fibers with soft and hard plastic coatings were loaded and photographed to depict which portion of the fiber (i.e., the core or cladding or the buffer coating) had been damaged. Corning fibers with soft acrylate coatings and fibers with hard polyimide coatings were evaluated. This testing indicated that severe damage would occur in both the soft and hard coatings, eventually causing the fiber to fracture. One interesting phenomenon that occurred during this testing phase was that the system hysteresis encountered during loading-unloading cycles decreased with an increasing number of cycles. However, a maximum of about 10 load-unload cycles caused failure of the fiber during this type of loading (*2*). It was concluded that the degradation of the buffer coating and stretching of the fiber were major causes of system hysteresis.

To study system hysteresis further, a sensor configuration that would prevent slippage and damage and that minimized fiber stretching was developed. A sensor in which the optical fiber was subjected to only two microbends was developed (Figure 4). The center-to-center rod spacings were fixed such that the fiber would not be overstressed in bending. Lindsay and Paton (*7*) suggest a breaking radius for Corning fiber from 0.8 to 1.5 mm [31 to 59 mils (1 mil = 10^{-3} in.)]. This range is the minimum radius allowed to prevent bending failure. On the basis of the recommendation of Lindsay and Paton (*7*), center-to-center rod spacings from 4.0 to 7.5 mm (157 to 295 mils) were used. The rods were used to firmly hold the fiber in place by controlling the distance between

Legend depicting numbers on figure

1. Deformable upper plate causes fiber microbending
2. Rigid spacers or sidewalls
3. Rigid or deformable base plate
4. Deformers such as metal or plastic rods
5. Springs
6. Rigid stopper to prevent excessive deflection
7. Optical fiber

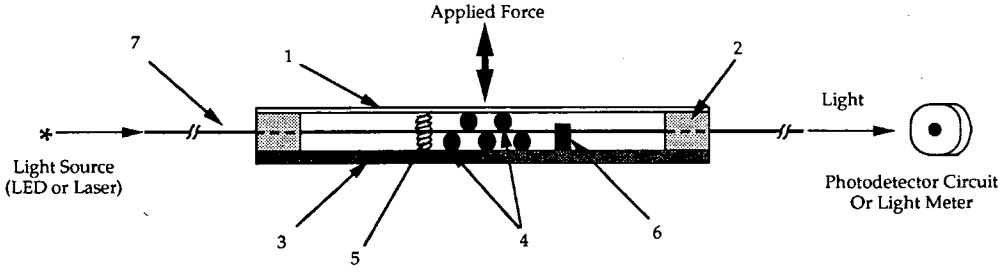

FIGURE 4 Microbending bridge architecture sensor (not to scale).

the sensor's top and bottom plates (Figure 4). This spacing enabled the optical fiber to be subjected to varying amounts of preliminary microbends (i.e., a small preloading was applied to the fiber), which allowed the linear range of the sensor's calibration curve to be used for testing.

BRIDGE ARCHITECTURE SENSOR

On the basis of the results from the testing described above, a microbend sensor called the bridge architecture sensor (BAS) was developed. A top plate was fixed to the bottom plate (Figure 4) so that it behaved like a beam with fixed end conditions. This configuration has the advantage that on release of load, the elastic beam action of the top plate enables the fiber to spring back to its original position. Springs may also be used because the top plate is relatively thin and it may not return to its original location after loading. A rigid stopper was added to prevent excessive deformation of the top plate (Figure 4). By changing the diameter and spacing of the rods and the dimensions of the top plate, five variations of this sensor were constructed. Table 1 summarizes the sensor configurations used. Corning 50/125/250-μm (1.97/4.92/9.8-mil) fiber was used for all BAS configurations (*2*).

BAS1 (Table 1) was tested by using the compression machine (Figure 2). Figure 5(*a*) shows applied load versus percent light output curves for a typical test. There was a maximum variation of about 5 percent between the increasing and the decreasing loads within the trial. The graph can be represented by using the third-order polynomials shown on the plot, with the regression coefficients indicating an excellent fit (*2*). Figure 5(*b*) shows that a linear relationship exists between the applied load and the percent light output from about 0.5 kg (1 lb) to 1.5 kg (3.3 lb), and again, the regression coefficient indicates an excellent fit. On the basis of this linear region, studies that concentrated on developing a linear load versus loss in light output intensity as the working range for the sensor were undertaken. By properly positioning the top and bottom plates to apply a preloading of approximately 0.5 kg (1.0 lb), the beginning of the linear portion [Figure 5(*b*)] would correspond to the beginning of working range. Numerous tests were conducted with BAS sensors preloaded in this manner, and the calibration plots all resembled the linear portion of Figure 5(*b*), with similar regression coefficients. When numerous load-unload cycles were performed with one sensor, the calibration curves were relatively consistent. Figure 6 shows the results from 15 load-unload cycles on BAS1 (*2*). There was a maximum variation within trials of about 5 percent and a change in response between the 1st and 15th trials of about 10 percent. The change in response between trials tended to decrease with increasing numbers of trials. The 5 percent variation is typical of results obtained for the BAS sensors. It represents the system hysteresis of the sensor, as was explained above. The exact cause of the 10 percent change from the 1st to the 15th trials is unknown. However, neither the material properties nor the bending characteristics of the sensor have been analyzed, and preliminary calculations by Kumar (*2*) indicate that the sensor top plate may be strained beyond acceptable elastic limits.

Increasing the rod diameters and, consequently, the rod spacings for BAS2 and BAS3 enabled a study of the variations of output light intensity and loads as a function of rod spacing. Comparison of the load versus light intensity test results for BAS1, BAS2, and BAS3 shows that increases in the rod diameter or spacings cause the load range over which the sensor is used to increase (Figure 7). Therefore, the sensors can be made less sensitive. This behavior was anticipated, since larger-diameter rods result in less bending of the fiber. For a 20 percent loss in output light, the load range was approximately 0.6 kg (1.25 lb), 1.8 kg (4.0 lb), and 3.0 kg (6.6 lb for BAS1, BAS2, and BAS3, respectively. The maximum variation in load within trials for all three sensor variations was about 5 percent (*2*). This portion of the research showed that it would be feasible to construct fiber optic sensors for specified load ranges by varying the rod diameters and spacings.

Tests were performed to study the effect of changes in sensor length on load range for the bridge architecture sensor. Sensors BAS2, BAS4, and BAS5 were used for this comparison. Figure 8 shows typical applied load versus percent light output for these sensors. For a 20 percent loss of output light, the load ranges for BAS2, BAS4, and BAS5 were approximately 1.8 kg (4.0 lb), 2.4 kg (5.2 lb), and 3.4 kg (7.5 lb), respectively (*2*). These results indicate that the load range increases as the length of the top plate is reduced. This behavior was expected, since the top plate's stiffness increases with a reduction in its length. Thus, more force is required to produce the same deflection of a shorter plate. This portion of the research showed that it would be feasible to construct fiber optic sensors for specified load ranges by varying the length of the top plate.

BAS2 was sealed and tested in the pressure chamber (Figure 2). A latex compound was used as the sealant; however, sealing this configuration proved to be very difficult because of the sen-

TABLE 1 Variations in BAS

Sensor Number	Top Plate Dimensions			Bottom Plate Dimensions			Rod	
	Length (mm)	Width (mm)	Thickness (mm)	Length (mm)	Width (mm)	Thickness (mm)	Diameter (mm)	Spacing (mm)
1	70	6.35	0.86	70	12.7	0.86	1.65	4.0
2	70	6.35	0.86	70	12.7	0.86	2.4	5.8
3	70	6.35	0.86	70	12.7	0.86	3.2	8.0
4	38.1	6.35	0.86	70	12.7	0.86	2.4	5.8
5	50.8	6.35	0.86	70	12.7	0.86	2.4	5.8

25.4 mm = 1 inch

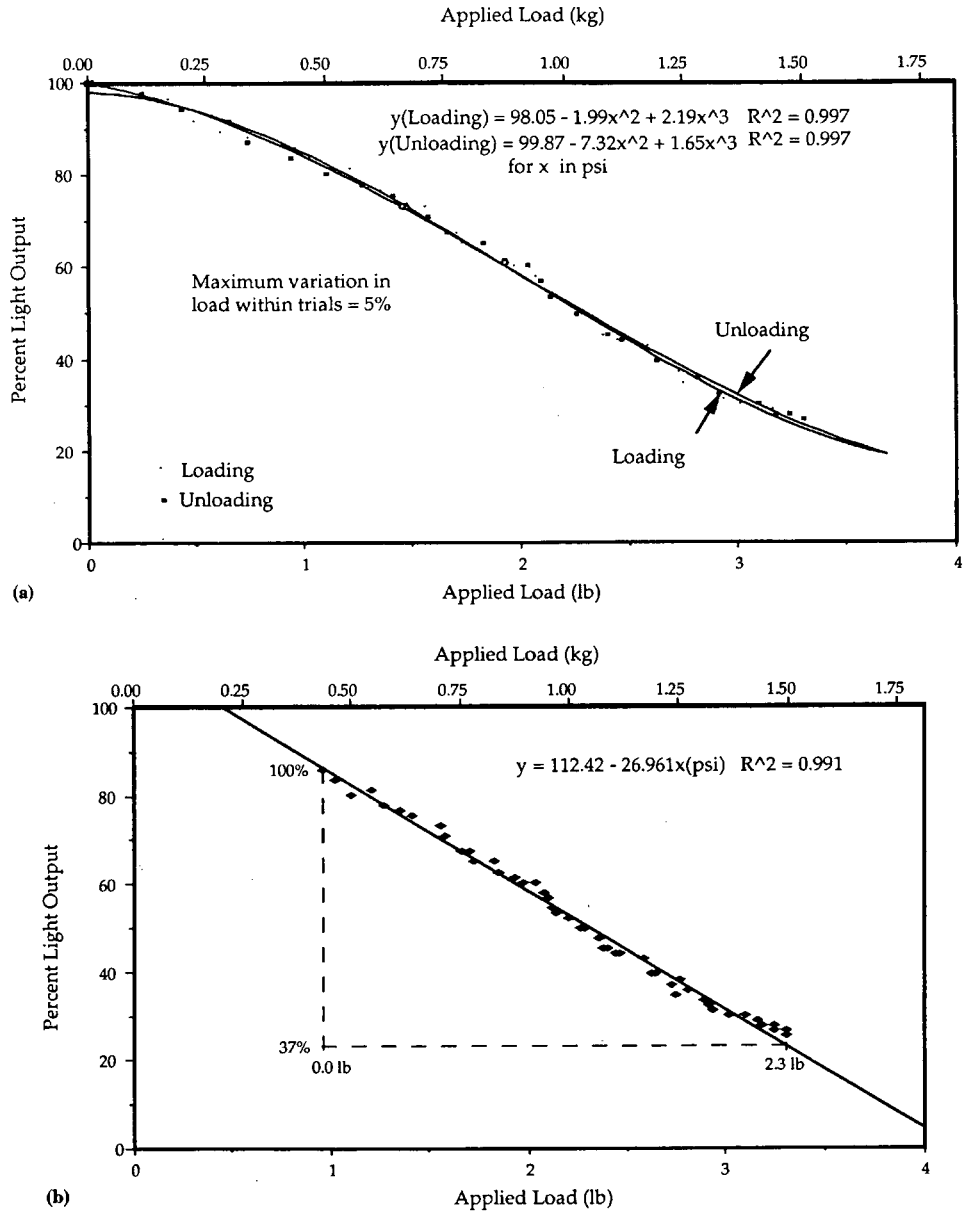

FIGURE 5 (*a*) **Applied load versus percent light output for a typical bridge architecture sensor.** (*b*) **Load range for linear region of** (*a*).

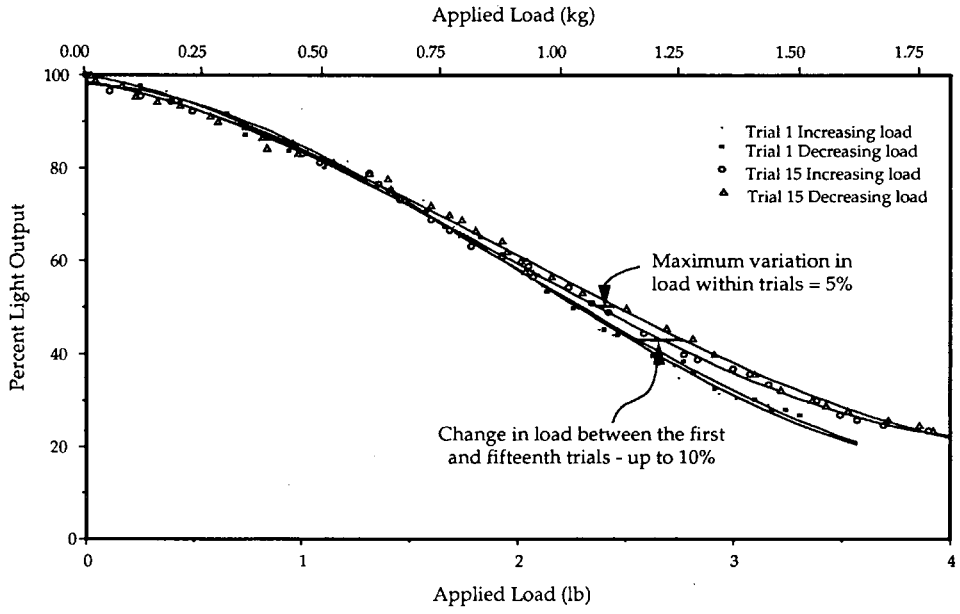

FIGURE 6 Applied load versus percent light output for the 1st and 15th trials for BAS1.

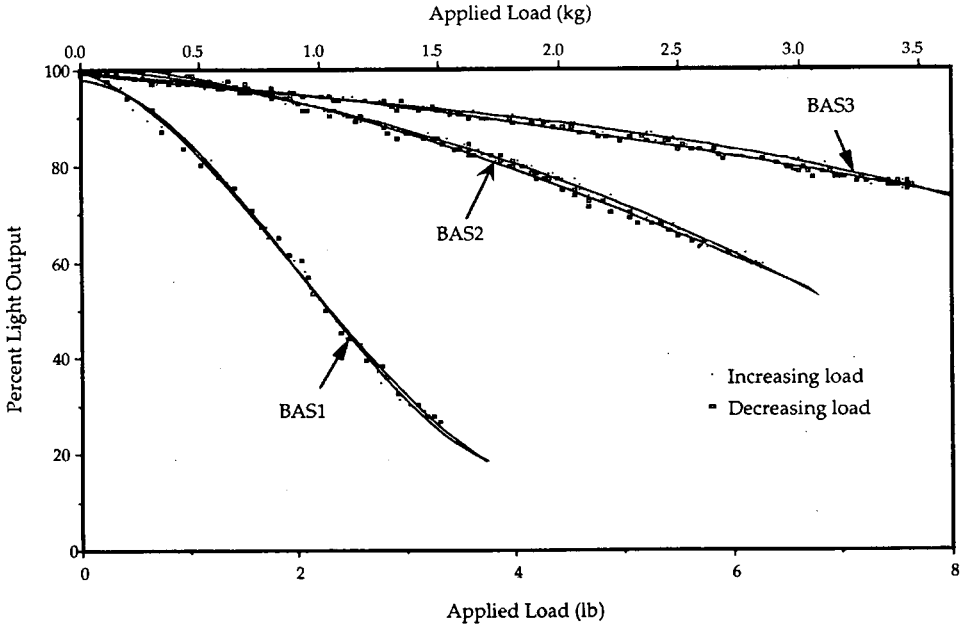

FIGURE 7 Variation in load range for the BAS with three rod diameters.

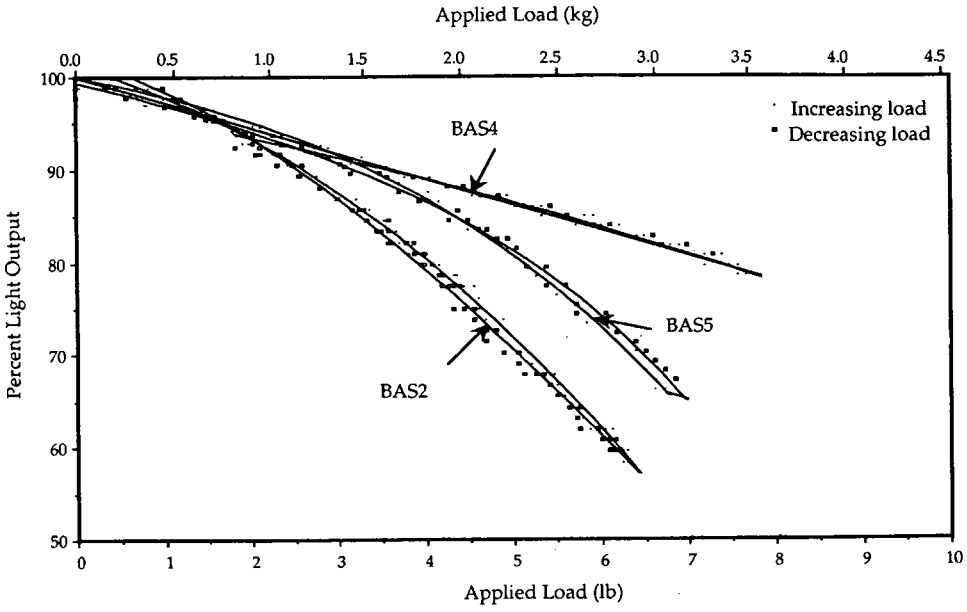

FIGURE 8 Variation in load range for the BAS with three top plate lengths.

sor's open sides. Figure 9(*a*) is a typical plot of the applied pressure versus percent light output. The initial portion of this curve is nonlinear; therefore, third-order polynomial regression equations were used to show that relationship between the data. The regression coefficients for these two curves indicate an excellent correlation between the parameters. The curve fit shown in Figure 9(*b*) depicts that a precise linear relationship could be achieved between the applied pressure and the percent light output from about 18 to 47 psi (125 to 325 kPa). This linearity is similar to that shown in Figure 5(*b*). Note that only one equation was used for the data depicted in Figure 9(*b*) since the datum points for the increasing and decreasing loads coincided. The similarity of these plots to Figures 5(*a*) and (*b*) indicates that the latex and epoxy sealants do not adversely affect the sensor's capabilities (*2*).

DISK ARCHITECTURE SENSOR

The results from BAS testing led to the development of a cylindrical sensor with the same basic configuration as those of BAS sensors. This configuration, termed the disk architecture sensor, is shown in Figure 10. The circular shape is simpler to seal, more robust, and therefore better than the BAS configuration for in situ applications. The disk sensor used for testing was constructed with the proper amount of preloading to eliminate the initial nonlinear portion of the calibration curve. This sensor was tested up to 100 psi (700 kPa) in the pressure chamber (Figure 2). Figure 11 shows the results from the increasing and decreasing pressure tests. A linear regression was used to represent both sets of data, and the regression coefficients for each line again indicate an excellent correlation between the two parameters. There is a maximum variation of about 4 psi between the increasing and decreasing pressure lines. This variation is the system hysteresis, and techniques to eliminate it are currently being investigated. Numerous load-unload trials were performed on this sensor, and the results from those tests indicate that the sensor gives repeatable results (*8*).

CONCLUSIONS

- Laboratory fiber optic sensors that can be used to measure loads of up to 2.2 kg (5 lb) and pressures of up to 700 kPa (100 psi) have been developed. Various configurations of BASs have been tested to show how the sensor construction affects the results. The BAS configuration was tested under loads from 0 to 2.2 kg (0 to 5 lb) and pressures from 0 to 415 kPa (0 to 60 psi). A disk architecture sensor configuration was tested, and it showed excellent results for pressures of from 0 to 700 kPa (0 to 100 psi). This configuration is preferred for use as a pore water pressure sensor because it is easier to seal and use in situ than the BAS configuration.
- The fiber optic sensor concept of microbending was studied, and problems of fiber damage and slippage were alleviated. Fiber damage can be prevented by ensuring that the fiber's bending radius is sufficient to prevent tensile cracks of the cladding and core. Slippage can be prevented and system hysteresis can be minimized by constructing microbend sensors with a small preloading of the fibers.
- There are still problems associated with system hysteresis. The hysteresis was minimized by applying loads directly to the fiber, which was placed against a metal plate; however, this type of loading resulted in premature fiber breakage. There is a maximum 4 percent change in the calibration curve during loading and unloading of a sensor. Hysteresis may be reduced by limiting the range of loading to a certain percentage of the sensor's maximum rated pressure value. However, since neither the material properties nor the bending characteristics of the sensor have been analyzed, this statement is only conjecture.

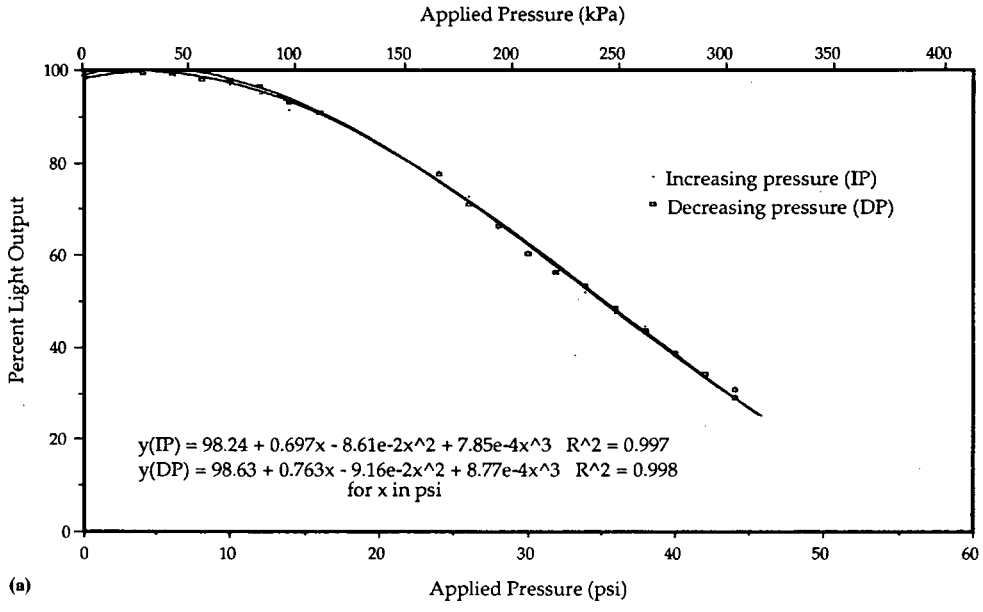

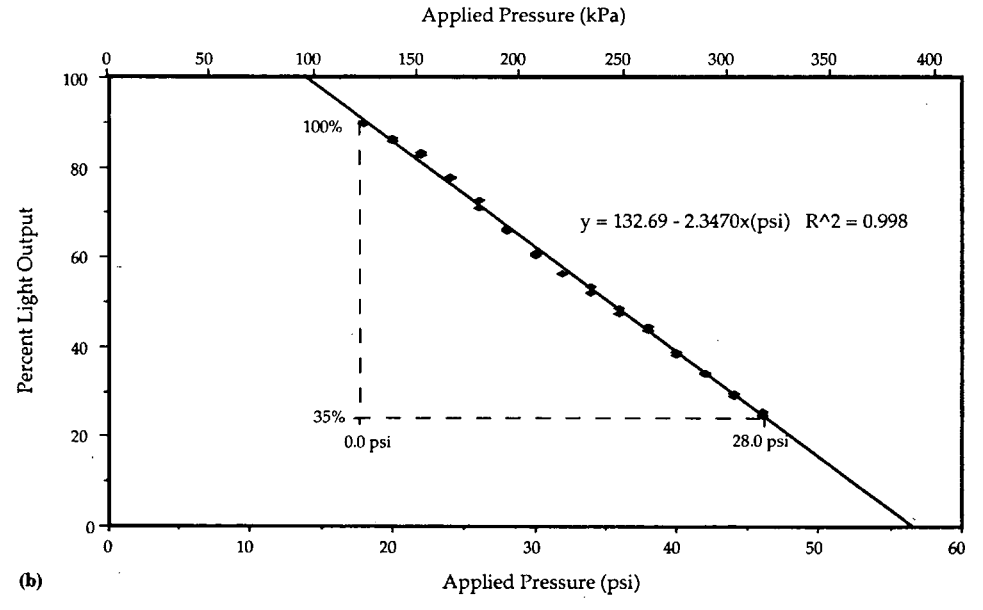

FIGURE 9 *(a)* **Typical applied pressure versus percent light output for latex-coated BAS2.** *(b)* **Linear pressure range for BAS2. Note that the equation of the line is based on both loading and unloading data.**

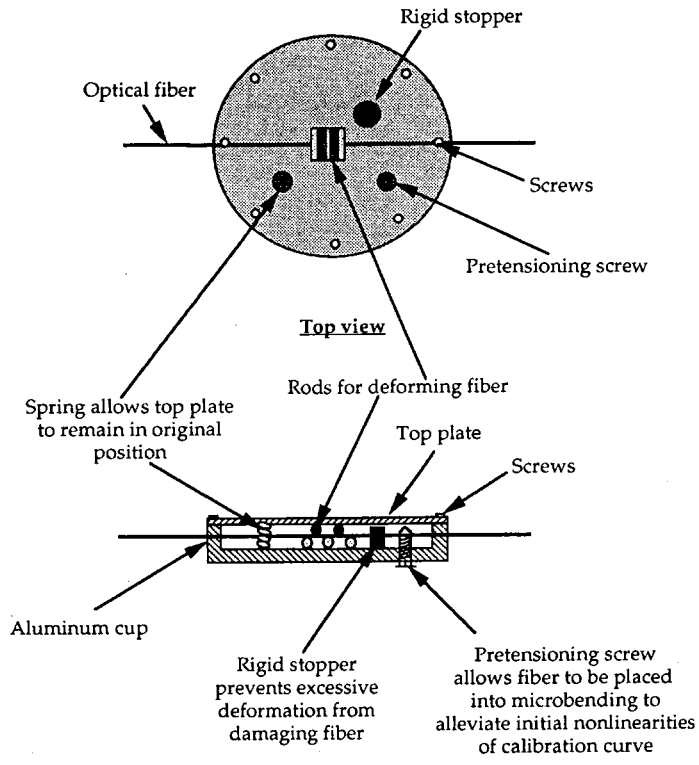

FIGURE 10 Disk architecture sensor (not to scale).

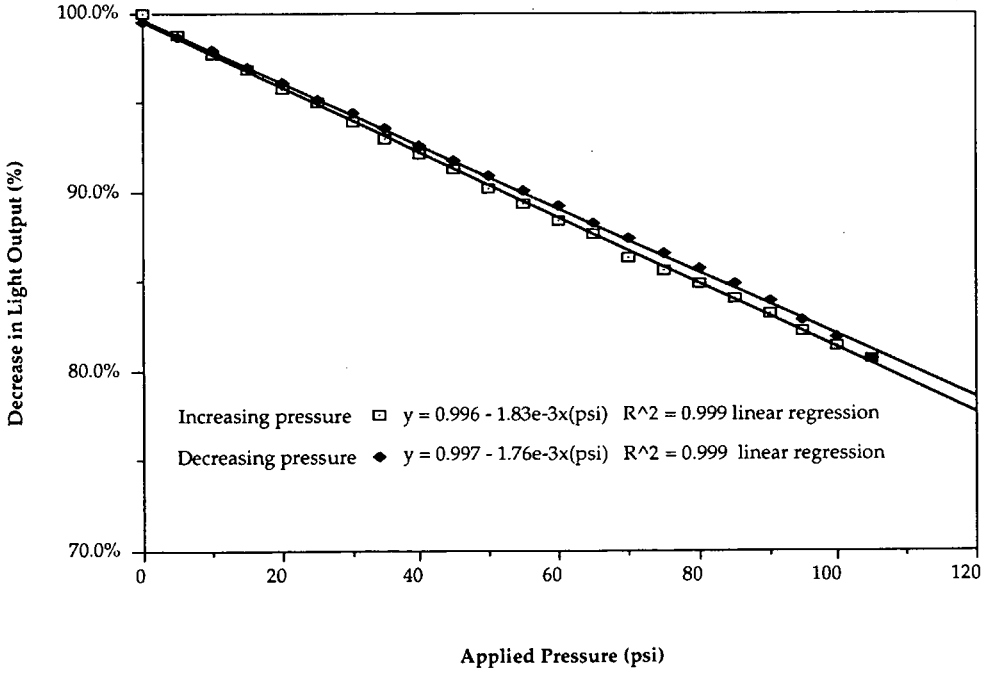

FIGURE 11 Pressure calibration for disk architecture sensor (1 psi = 6.9 kPa).

• The microbend sensors have been studied and calibrated by using a load-pressure calibration system that can be used to test microbend sensors for loads of up to 454 kg (1,000 lb) and pressures in excess of 700 kPa (100 psi).

RECOMMENDATIONS

Recommendations for future work include the following.

• Studies of the sensor's material properties during prolonged usage are needed. These studies would involve short- and long-term static, dynamic, and chemical analyses of the optical fiber and brass or plastic materials used to form the sensor.
• Studies of the system hysteresis, which is still occurring, must be completed. It is recommended that a number of microbending tests be conducted to determine the bending characteristics of the fiber.
• Studies of the potential range of pore pressures over which either BAS or disk architecture sensors can be used must be completed.
• Once the laboratory phase of the research is completed, in situ testing at instrumented field sites should be conducted.

ACKNOWLEDGMENTS

The researchers would like to thank the Florida Department of Transportation for funding this research. The assistance of Joe Caliendo and Peter Lai throughout the study was invaluable. This publication has been prepared in cooperation with the Florida Department of Transportation and the U.S. Department of Transportation.

REFERENCES

1. Dunnicliff, J. *Geotechnical Instrumentation for Monitoring Field Performance*. John Wiley and Sons, Inc., New York, 1988.
2. Kumar, G. *Developing a Fiber Optic Pore Pressure Sensor*. M.S. thesis. Florida Institute of Technology, Melbourne, 1993.
3. Nanni, A., C. C. Yang, K. Pan, J.-S. Wang, and R. R. Michael, Jr. Fiber-Optic Sensors for Concrete Strain/Stress Measurement. *ACI Materials Journal*, Vol 88, No. 3, May–June 1991, pp. 257–264.
4. Baker, D. G. *Fiber Optic Design and Applications*. Reston Publishing Co., Reston, Va., 1985.
5. Kim, B. Y., and H. J. Shaw. Multiplexing of Fiber Optic Sensors. *Optic News*, Nov. 1989, pp. 35–42.
6. Wolfbeis, O. S. Novel Techniques and Materials for Fiber Optic Chemical Sensing. *Optic Fiber Sensors*, Springer-Verlag, Berlin, 1989, pp. 416–424.
7. Lindsay, K. E., and B. E. Paton. Wide Range Optical Fiber Microbending Sensor. *Optical Testing and Metrology*, Vol. 661, 1986, pp. 211–217.
8. Cosentino, P. J., and B. G. Grossman. *Developing Fiber Optic Sensors to Measure Pore Water Pressures*, Final Report. Contract No. C-4516, Florida Department of Transportation, Jan. 1994.